Research Article | Vol. 13, No. 4 / 1 Apr 2022 / Biomedical Optics Express 1948

Biomedical Optics EXPRESS

Effect of decentration, tilt and rotation on the optical quality of various toric intraocular lens designs: a numerical and experimental study

JESÚS PÉREZ-GRACIA, JORGE ARES, FRANCISCO J. ÁVILA, AND LAURA REMÓN*

Departamento de Física Aplicada, Universidad de Zaragoza, Zaragoza, Spain
**lauremar@unizar.es*

Abstract: Toric intraocular lenses (T-IOLs) may lose their optical quality if they are not correctly positioned inside the capsular bag once implanted. In this work, T-IOLs with cylinder powers of +1.50, +4.50 and +7.50 D and differing degrees of spherical aberration have been designed, manufactured and tested *in vitro* using a commercial optical bench that complies with the requirements of standard ISO 11979-2. Moreover, the effect of tilt and rotation on optical quality was assessed by means of numerical ray tracing on an astigmatic eye model, while the effect of decentration was evaluated numerically and experimentally.

1. Introduction

The availability of toric intraocular lenses (T-IOLs) on the market since the 1980s [1] has allowed the complete correction of corneal astigmatism simultaneously with cataract surgery, thus allowing these patients to achieve complete independence from refractive correction [2]. The first clinical study collecting the postoperative results of T-IOL implantation dates from 1994 [3]. That first T-IOL was a three-piece poly (methyl methacrylate) lens that required a corneal incision of 5.7 mm for implantation. However, in the early 1980s, the T-IOL was additionally intended to correct the surgically induced astigmatism [4] caused by large corneal incisions [5]. Since the introduction of the first foldable single-piece T-IOL made of silicone in 1994 [6], the materials used in IOLs have been evolving, thus allowing smaller corneal incisions and minimally invasive surgical techniques. Nowadays the market offers a wide range of T-IOLs, classified by their raw material [7], optic design [8], haptic design [9], and cylinder dioptric power [10].

Regardless of the different characteristics of IOLs, biomechanical stability is a key part of achieving satisfactory vision correction in patients. Rotation is the principal complication of the T-IOL and causes residual astigmatism that affects optical performance [11,12]. However, in addition to T-IOL rotation producing a reduction in optical quality, decentration and tilt also have a detrimental effect. Clinically, the study performed by Mihály *et al.* [13] compared refractive outcomes after implantation of two types of T-IOLs in patients with corneal astigmatism prior to cataract surgery. The T-IOL with lower average postoperative rotation ($3.00 \pm 2.26°$) obtained refractive outcomes closer to emmetropia, compared to the T-IOL with a higher average rotation ($3.27 \pm 2.37°$). Several studies have evaluated the optical performance of different currently marketed T-IOLs, and its degradation with misalignment, experimentally [8,14,15] and numerically [16]. Thus, Kim *et al.* [8] designed an optical bench to evaluate the effect of degree of IOL decentration and rotation on the image quality of four commercial aspheric T-IOLs. The T-IOLs used in that study had different designs (transitional conic toric; bitoric IOL; posterior toric surface IOL and anterior toric surface IOL) and a spherical-equivalent (SE) and cylinder power that varied between these designs, thus making comparison of the findings cumbersome. Tognetto *et al.* [14] evaluated the image quality obtained with the same T-IOL (SN6AT6, Alcon Laboratories, Inc.) for different rotational angle errors experimentally. This T-IOL presents a

#447045 https://doi.org/10.1364/BOE.447045
Journal © 2022 Received 28 Oct 2021; revised 21 Feb 2022; accepted 26 Feb 2022; published 8 Mar 2022

Biomedical Optics EXPRESS

negative spherical aberration (SA) with an SE of +21.00 D and a cylindrical power of +3.75 D to correct a 3.00 D corneal astigmatism. Their findings demonstrated that a rotation of 15.00° causes a moderate visual quality loss, while a severe visual quality loss occurs for rotations up to 30.00°. Pérez-Vives *et al*. [15] studied the optical quality of the same design of commercial T-IOLs (SN6AT with a negative SA) with decentrations experimentally. They evaluated T-IOLs of different SE powers (+15.00, +20.00 and +23.50 D) with different cylinder powers (1.50, 2.25 and 3.00 D). The decentrations analyzed were 0.3 and 0.6 mm, and the authors found a substantial decrease in the *modulation transfer function* (MTF) with the highest decentration. Zhang *et al.* [16] evaluated the optical performance of a T-IOL and a spherical monofocal IOL after decentration (decentered from 0.25 to 0.75 mm) using a theoretical model eye. They concluded that the tolerance of the T-IOL analyzed to decentration was similar to a spherical monofocal IOL.

The heterogeneity of theoretical (different eye models) and experimental (different optical benches) methods, and the fact that only one T-IOL model per eye is considered, make the comparison of results cumbersome. Moreover, the standard ISO 11979-2 [17] specifies the use of a spherical cornea model to obtain the optical quality of T-IOLs, differing from normal conditions once the lens has been implanted in a real eye.

The aim of this study is to accomplish a comprehensive analysis of the image quality offered by different aspheric T-IOLs. As such, T-IOLs with different degrees of SA and different cylinder powers with the same SE have been designed and the effect of decentration, tilt and rotation on the image quality of a modified eye model has been assessed numerically. In this study the Atchison eye model [18] was used and its anterior surface was modified to achieve an astigmatic eye model that could be completely corrected by the toric IOL. Moreover, the T-IOL designs have been manufactured and evaluated using a commercial optical bench (PMTF system) that complies with the methods specified in the standard ISO 11979-2 [17]. Although several studies [8,14,15] evaluated the optical performance experimentally *in vitro*, these studies used T-IOLs present on the market, the designed aspheric surfaces of which are not known and with different SAs, thus making comparison of the results difficult.

2. Materials and methods

2.1. Eye model

In order to design T-IOLs and to evaluate the effect of decentration, tilt and rotation on optical performance, a numerical model of a pseudophakic eye was implemented and analyzed using numerical ray tracing and commercial optical design software (Zemax, OpticStudio 21.2.1). The pseudophakic eye model was based on the Atchison model eye [18], selecting a spectacle mean spherical refraction of 0.00 D, and replacing the eye lens with a particular IOL for each case studied (see Table 1 for details). The position of the iris was 2.72 mm from the posterior corneal vertex and the initial position of the IOL within the pseudophakic eye model was set so that its anterior vertex was at a distance of 4.5 mm from the posterior corneal surface, according to an effective lens position in pseudophakic eyes [19,20]. The cornea of the eye model has a refractive power of +42.48 D, and a fourth-order Zernike (Z_4^0) standard ANSI (American National Standard Institute) SA of +0.250 µm for a 6.00 mm entrance pupil diameter (5.45 mm iris diameter) [18]. A biconical cornea with a horizontal X meridian based on the data from Atchison's eye model (see Table 1) and the vertical Y meridian adjusted for each model of T-IOL to present the opposite astigmatism to the IOL, and to keep the same amount of spherical aberration as the model eye, was designed (see Table 2 for details).

Biomedical Optics EXPRESS

Table 1. Eye model used for toric IOL designs and simulations [18].

Surface	X Meridian		Y Meridian		Thickness (mm)	Refractive index at 550 nm
	Radius (mm)	Conic Constant	Radius (mm)	Conic Constant		
Anterior cornea	7.77	-0.150	To be determined according to IOL design[a]		0.55	1.3760
Posterior cornea	6.40	-0.275	6.40	-0.275	2.72	1.3374
Pupil	Infinite	—	Infinite	—	1.78	1.3374
IOL anterior surface	To be determined according to IOL design[a]		To be determined according to IOL design[a]		0.9	1.4600
IOL posterior surface	-25.3	0.000	-25.3	0.000	To be determined according to IOL design[b]	1.3360
Retina	-12.0	0.260	-12.0	0.260		

[a]The anterior cornea surface and the IOL's anterior surface have a different radius and conic constant data for the vertical Y meridian. See Table 2.
[b]See Table 2.

2.2. Toric intraocular lens design

T-IOL models with a spherical equivalent (SE) of +20.00 D were designed with three different cylinder (CYL) values of +1.50, +4.50 and +7.50 D, which were used to correct a corneal astigmatism of +0.99, +2.96 and +4.94 D, respectively. T-IOLs were designed to be manufactured in hydrophilic acrylic material (Benz IOL 25 Universal Blank; refractive index n = 1.460 at the design wavelength $\lambda_0 = 550$ nm). The toric surface of the IOLs was placed in the anterior surface of the lens (see more details of the radius of curvature in Table 2). The central thickness was 0.9 mm, and the radius of curvature for the back surface was -25.3 mm for all lenses.

Two types of aspherical lenses were designed for each cylinder power using biconical anterior surfaces: Lens A was a T-IOL with fourth-order Zernike-negative SA to totally compensate the fourth-order Zernike-positive SA of the Atchison cornea, and Lens B was designed as a T-IOL that does not add any fourth-order Zernike SA to the Atchison cornea. As both T-IOLs have different asphericities at each meridian of the anterior surface (see Table 2 for details), they are referred to as atoric Lens A and atoric Lens B in accordance with the literature [21]. The optical design involved optimization of the conic constant for each corresponding main meridian of the lens anterior surface to achieve the fourth-order Zernike coefficient (Z_4^0) [22] for each design. For comparison, T-IOLs with the same spherical equivalent and cylinder power, with their corresponding anterior toric surfaces, were designed and evaluated. These lenses are referred to as classical toric lenses.

To study the optical quality provided by each IOL design placed inside its best corresponding typical astigmatic eye, several astigmatic biconical corneas were designed to match three conditions: 1) Maintain the corneal horizontal meridian with the same geometry as Atchison's cornea model, 2) Maintain the same corneal fourth-order SA as Atchison's cornea model, 3) Cancel the nominal IOL astigmatism, so the astigmatism of the whole eye was zero when the IOL was in a centered position. Further details of the geometry of these astigmatic model corneas and each corresponding T-IOL design can be found in Table 2. In addition, for each T-IOL design, the vitreous camera depth was set to achieve the maximum MTF volume by numerical integration from 0 to 100 cycles/mm, following a similar criterion to that studied by Guirao and Williams [23]. Taking into account that we are keeping the horizontal corneal meridian geometry and

Table 2. Parameters for the anterior surface of the toric IOLs used in the simulations and experiments. Radius of curvature and conic constant for the vertical Y meridian of the corneal eye model.

IOL Power (SE = +20 D)	Y meridian of the eye model anterior cornea[a]		IOL anterior radius (mm) [Shape factor][b]		IOL Design	Conic constant		IOL SA (μm) (Ø iris 3 mm)	Vitreous chamber thickness[c] (mm)
	Radius (mm)	Conic constant	X	Y		X	Y		
+1.50D CYL	7.941	-0.132	8.615 [+0.492]	7.800 [+0.528]	Atoric Lens A	-4.20	-4.00	-0.021	18.42
					Atoric Lens B	-0.76	-0.54	0.000	18.32
					Classical Toric	0.00	0.00	+0.005	18.30
+4.50D CYL	8.316	-0.086	9.621 [+0.448]	7.125 [+0.560]	Atoric Lens A	-5.79	-2.02	-0.021	18.83
					Atoric Lens B	-0.93	-0.42	0.000	18.75
					Classical Toric	0.00	0.00	+0.004	18.73
+7.50D CYL	8.735	-0.043	10.893 [+0.398]	6.558 [+0.588]	Atoric Lens A	-8.32	-1.48	-0.021	19.27
					Atoric Lens B	-1.23	-0.28	0.000	19.18
					Classical Toric	0.00	0.00	+0.005	19.16

[a]Data for the X meridian curvature radius and conic constant of the eye model anterior cornea can be found in Table 1.
[b]The values in square brackets in the IOL radius parameters represent the shape factor of the T-IOLs at the X and Y meridians. The shape factor is calculated as $(R_{\text{posterior radius}}+R_{\text{anterior radius}})/(R_{\text{posterior radius}}-R_{\text{anterior radius}})$.
[c]Distance between IOL posterior surface vertex and retina.

Biomedical Optics EXPRESS

corneal SA with the same value for all cases, vitreous depth values will change according to the astigmatism and SA of each particular IOL. Table 2 also shows the SA of each IOL for a 3.00 mm iris diameter.

Finally, all T-IOL designs were manufactured following a lathe-milling technique. Differences between the theoretical design and the manufactured IOL profiles were lower than 1 µm, as measured using a contact profilometer (DEFTA kXT, Bruker).

2.3. Numerical simulations

Once each T-IOL had been designed (see Table 2), its optical performance was evaluated inside the eye model using the optical design software Zemax for different alignment conditions of the lenses.

Initially, the T-IOLs were decentered from 0.00 mm (on-axis position) to 1.00 mm, in 0.25 mm steps, relative to the pupil center. In the eye model, the iris center and the cornea optical axis were aligned. The IOL decentrations were performed in both axes: horizontal (X-axis) and vertical (Y-axis). Secondly, the T-IOLs were tilted relative to the corneal optical axis, maintaining the IOL anterior vertex in the pupil center. The tilt range analyzed was from 0.00° (untilted IOL) to 5.00°, in 1.00° steps, and once again, this performed in both axes. Finally, the toric IOLs were rotated from their nominal position to 15.00°, in 5.00° steps. The rotation was performed in positive (clockwise) and negative (counter-clockwise) directions.

For each decentration, tilt and rotation, the MTF in both meridians (MTF-Y and MTF-X) at 100 cycles/mm for a 3.00 mm iris diameter (3.35 mm entrance pupil) was calculated following the procedure described in the standard ISO 11979-2 [17] and compared to 0.43, i.e., the minimum MTF values established in ISO 11979-2 [17], to determine whether a manufactured T-IOL offers an adequate optical imaging quality at each meridian. Apart from the MTF analysis, the Zernike wavefront aberration coefficients associated with defocus (Z_2^0), astigmatism (Z_2^{-2} and Z_2^2), and primary coma (Z_3^{-1} and Z_3^1) were computed for a wavelength of 550 nm. The root mean square (RMS) was calculated for the described aberrations at each decentration, tilt and rotation for all lenses.

In addition, for the sake of completeness, the spherocylindrical refraction for minimum RMS wavefront error of the model eye was calculated with a 15° rotation in the T-IOLs. To estimate this, the Zernike wavefront coefficients were needed, using the "refractive Zernike power polynomials" described in the study of Iskander *et al.* [24]. The following equations were applied to obtain the power vector components of the objective refraction M, J_0 and J_{45}:

$$\begin{aligned} M &= \frac{-Z_2^0 \cdot 4 \cdot \sqrt{3}}{r^2}; \\ J_0 &= \frac{-Z_2^2 \cdot 2 \cdot \sqrt{6}}{r^2}; \\ J_{45} &= \frac{-Z_2^{-2} \cdot 2 \cdot \sqrt{6}}{r^2} \end{aligned} \tag{1}$$

where (Z_2^0) is the defocus, $(Z_2^{-2}$ *and* $Z_2^2)$ the astigmatism in µ*m* and r is the radius of the pupil's system in *mm* where the Zernike coefficients were calculated. The following equations were also used to obtain the final refraction of the designed T-IOL with each astigmatic cornea:

$$\begin{aligned} Sph &= M - \frac{Cyl}{2}; \\ Cyl &= -2 \cdot \sqrt{(J_0)^2 - (J_{45})^2} \end{aligned} \tag{2}$$

2.4. Experimental measurements

The optical performance for all T-IOLs manufactured was tested experimentally *in vitro* using the PMTF optical bench (Lambda-X, Belgium), with software version V.2.4.1. This device follows

Biomedical Optics EXPRESS

the requirements specified in the standard ISO 11979-2 [17] for the measurement of T-IOLs. To obtain the MTF information, the setup uses the slanted edge MTF technique, which consists of imaging a slanted vertical or horizontal edge on the detector. A model biconvex spherical cornea manufactured in N-BK7 (refractive index n = 1.5168 at the wavelength $\lambda_0 = 550$ nm), with an anterior and posterior curvature radius of 51.22 mm and -28.00 mm, respectively, and a focal length of 36.10 mm, was used in the PMTF following the ISO specifications. The central thickness was 6.90 mm and the aperture diameter was 16.00 mm. The shape factor of this cornea was -0.29, providing a +0.295 µm SA for a +6.00 mm entrance pupil diameter. The reason for using this artificial cornea was the similarity of its SA aberration conditions with the +0.250 µm SA of Atchison's cornea model [18] used in the ray tracing simulation. Note that the artificial cornea used by the PMTF optical bench does not match the specifications of the cornea used in the numerical simulations (described in Tables 1 and 2).

In the PMTF optical bench, the illumination system consists of a collimated LED source with a center wavelength of 546 nm. The artificial eye is composed of an artificial cornea and a wet cell into which the IOL is inserted into a balanced salt solution (BSS Distra-Sol, Ophcon). Finally, a CCD camera (pixel size of 4.65×4.65 µm) is attached to an X20 microscope objective (in order to achieve a spatial effective resolution of 0.23 µm/pixel) to capture the images formed along the optical axis of the optomechanical eye model with the toric IOL under test. For more information regarding the PMTF optical bench, see the paper by Pérez-Gracia *et al.* [25].

In this experimental study, the MTF of both IOL main meridians (MTF-Y and MTF-X) was measured for decentrations from 0.00 to 1.00 mm in steps of 0.25 mm for all the T-IOL designs. Incidentally, the presence of astigmatism during the PMTF measurements due to the non-toric artificial cornea meant that the horizontal and vertical MTF behavior cannot be measured simultaneously using a unique axial position of the PMTF CCD detector. To overcome this, vertical and horizontal slanted edge tests were necessary to obtain the two foci of the toric IOLs, with axial scanning of the PMTF detector. As a consequence, during the measurements, only the MTF for one slanted edge test (vertical or horizontal) was taken into account for each respective decentration. Controlled lens decentration was achieved by means of the calibrated displacement of the PMTF X-Y translation stage. In addition, and according to standard ISO 11979-2, the through-focus MTF (TF-MTF) was measured at 100 cycles/mm, with a 3.00 mm iris diameter, for all T-IOLs in a centered position.

3. Results

3.1. Numerical results

The MTF analysis (MTF-Y and MTF-X) was performed with decentration (Fig. 1), tilt (Fig. 2) and rotation (Fig. 3) of the T-IOLs. The yellow background of the figures represents decentration and tilt through the vertical axis, and the negative direction for rotation measurement. The grey background shows decentration and tilt within the horizontal axis and positive rotation.

Figure 1 compiles the MTF results with decentration of the T-IOLs in the model eye. The results for each cylinder are shown. As expected, it can be seen that the MTF-Y and MTF-X values vary from horizontal to vertical decentration. However, the MTF values for each decentration direction are not symmetric for any of the lenses analyzed. In all cylinder diopters, the atoric Lens A showed the highest on-axis MTF, as it is an aberration-correcting IOL for that cornea, while the lowest value was obtained for the classical toric lens. The atoric Lens B had lower values than Lens A, as was expected due to its design for neutral aberration correction.

When the different decentration values were applied, both MTF values (MTF-Y and MTF-X) for the atoric Lens A decreased rapidly to values of less than 0.43, for a decentration value higher than 0.25 mm (mean between MTF-Y and MTF-X). The atoric Lens B was barely affected by decentration for all cylinder powers. For this design, the MTF-Y and MTF-X never decrease below 0.43 for any decentration. The classical toric lens behaved similarly to the atoric Lens B.

Biomedical Optics EXPRESS

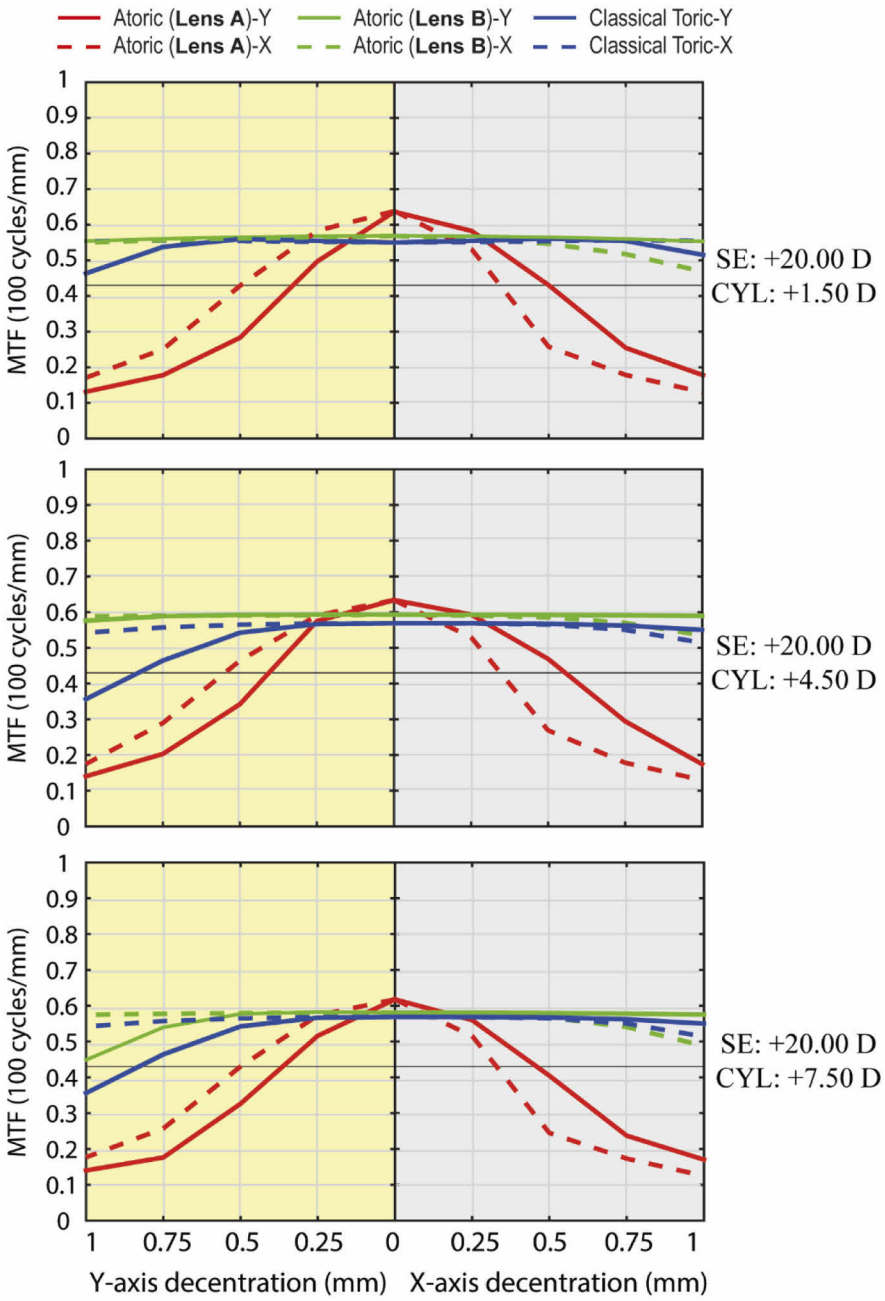

Fig. 1. Numerical MTF-Y (continuous line) and MTF-X (dashed line) values for the different T-IOL designs as a function of decentration, with a 3.00 mm pupil diameter and 100 cycles/mm for the different cylinder diopters. The yellow background represents a T-IOL decentration in the Y-axis direction, the grey background represents a decentration in the X-axis direction. The horizontal black line represents an MTF value of 0.43, the tolerance limit established in ISO 11979-2 [17].

Biomedical Optics EXPRESS

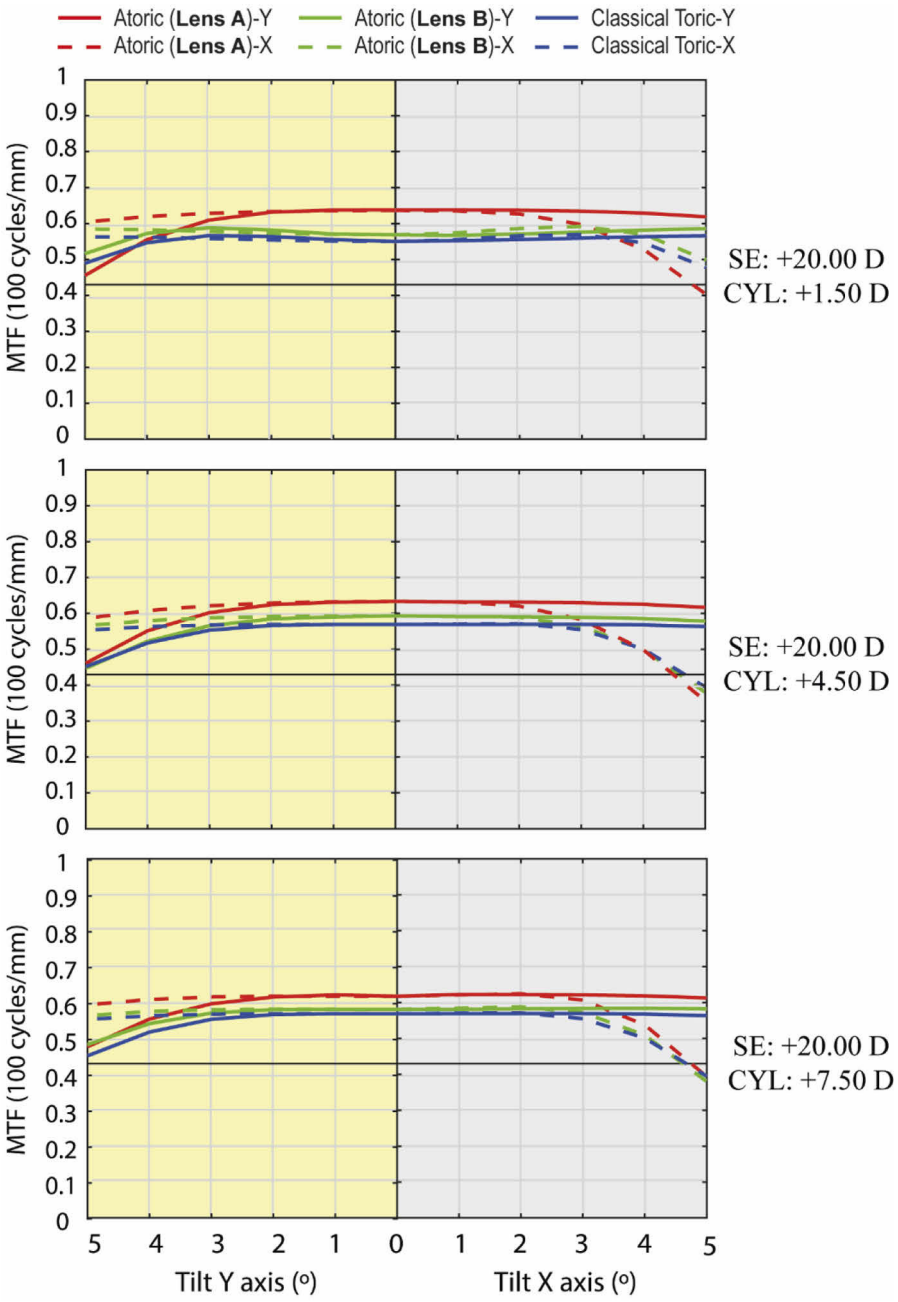

Fig. 2. Numerical MTF-Y (continuous line) and MTF-X (dashed line) values for the different T-IOL designs as a function of tilt, with a 3.00 mm pupil diameter and 100 cycles/mm for the different cylinder diopters. The yellow background represents a T-IOL tilt in the Y-axis direction, the grey background represents a tilt in the X-axis direction. The horizontal black line represents an MTF value of 0.43, the tolerance limit established in ISO 11979-2 [17].

Biomedical Optics EXPRESS

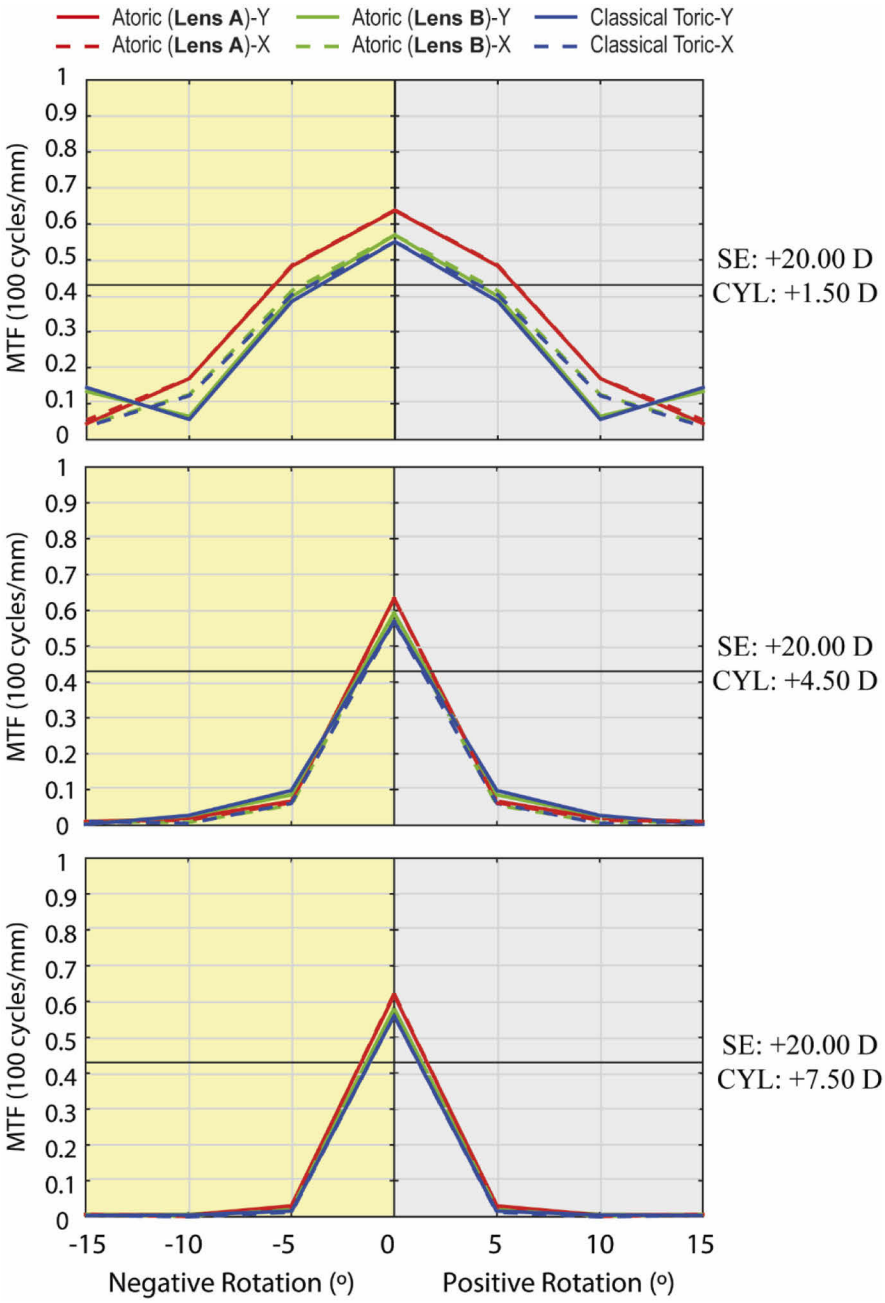

Fig. 3. Numerical MTF-Y (continuous line) and MTF-X (dashed line) values for the different T-IOL designs as a function of rotation, with a 3.00 mm pupil diameter and 100 cycles/mm for the different cylinder diopters. The yellow background represents a T-IOL rotation in the negative direction, the grey background represents a rotation in the positive rotation. The horizontal black line represents an MTF value of 0.43, the tolerance limit established in ISO 11979-2 [17].

Biomedical Optics EXPRESS

However, the MTF-Y values decreased to less than 0.43 for a decentration of more than 0.75 mm at cylinder powers of +4.50 and +7.50 D.

Figure 2 shows the MTF variation as a function of tilt for all cylinder powers. In this case, both MTF values (MTF-Y and MTF-X) were less dependent on the T-IOL design than for IOL decentration. Here, the most noticeable finding is that all lenses gave MTF values higher than 0.43 for all tilt values, except for a 5° tilt performed in the horizontal direction for lenses with a cylinder of +4.50 and +7.50 D.

Figure 3 shows the variation in MTF as a function of rotation for all cylinder powers. It is noticeable that the rotation is dependent on the cylinder power. Thus, for the +1.50 D cylinder, the atoric Lens A is the only T-IOL design whose MTF value drops below 0.43 for a rotation higher than 5° in both directions. The atoric Lens B and the classical toric lens gave MTF values of less than 0.43 for a rotation of 5°. For the cylinders +4.50 and +7.50 D, the MTF decreases drastically with rotation, giving an MTF of less than 0.1 with a rotation of 5° for all T-IOL designs.

Table 3 shows the sphero-cylindrical refraction error produced by the T-IOLs with a 15° rotation. These values are calculated using Eqs. (1) and 2. To compensate for the refractive error caused by a rotation of 15° in the T-IOLs of CYL +1.50 D, a cylinder of -0.60 D is needed, thus meaning that the loss of effectiveness of the T-IOL is around 40%. With the T-IOLs of CYL +4.50 D, the cylinder needed to compensate for the refraction error is -1.90 D, thus leading to a T-IOL effectiveness loss of 42%. With the T-IOL of CYL +7.50 D, the effectiveness of the astigmatism correction decreases to a total loss of 43% with a 15° rotation in the IOL. However, there is no difference between the T-IOL designs in terms of the refraction error for each CYL power. With regard to the variation of the spherical power refraction error, a noticeable increase is observed, with the increase in T-IOL requiring a greater sphere power correction as the cylinder power of the T-IOL increases.

Table 3. Sphero-cylindrical refraction error of the astigmatic cornea and T-IOL system with a 15° rotation of the T-IOL.

		Rotation: 15°		
T-IOL design		CYL: +1.50 D	CYL: +4.50 D	CYL: +7.50 D
Atoric (Lens A)	**Sphere**	0.31 D	0.96 D	1.63 D
	Cylinder	-0.60 D	-1.93 D	-3.23 D
Atoric (Lens B)	**Sphere**	0.36 D	0.95 D	1.61 D
	Cylinder	-0.64 D	-1.91 D	-3.21 D
Classical Toric	**Sphere**	0.35 D	0.95 D	1.60 D
	Cylinder	-0.64D	-1.92 D	-3.21 D

For the aberration analysis, the same background colours as the MTF figures have been used to represent decentration and tilt in the horizontal or vertical axis and a positive or negative rotation of the T-IOLs. The central area of the figure (white background) represents the on-axis aberration values.

Figures 4 and 5 show the RMS for decentration and tilt, respectively. In these figures, the first row shows the RMS defocus, the second row shows the RMS astigmatism and the third row shows the RMS coma. As the results obtained in the aberration analysis are very similar for all cylinders of the T-IOLs, for the sake of conciseness, only the results for the T-IOL designs with CYL +4.50 D are shown. In general, it can be seen that IOL decentration and tilt increase wavefront aberrations irrespective of the IOL design. A lower increase in coma aberration is obtained with tilt compared with defocus and astigmatism. For all the aberrations studied, the results for all lenses are not the same when applying the decentration or tilt in the horizontal direction (yellow background) compared with applying them in the vertical direction (grey background). This

Biomedical Optics EXPRESS

behavior is expected given that the horizontal and vertical directions correspond, respectively, with the direction of the main meridians of the IOL, in other words the x and y directions, respectively, correspond with the meridians with lower and greater power for the IOL.

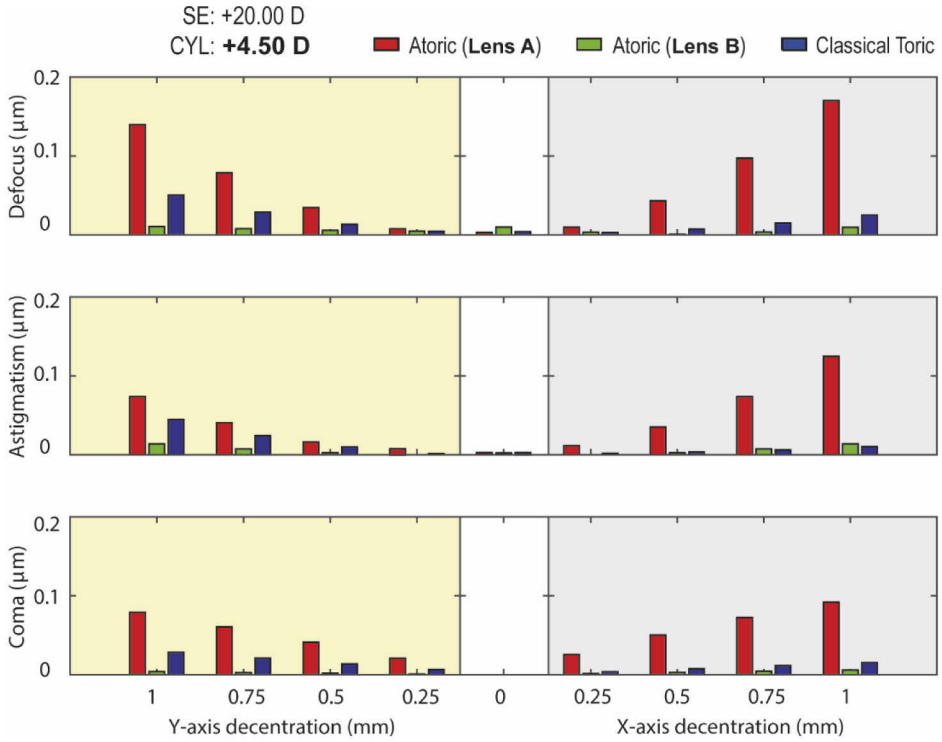

Fig. 4. Numerical results for RMS defocus, astigmatism and coma for decentrations with the different T-IOL designs and a +4.50 D cylinder, measured with a 3.00 mm diameter pupil. The white background represents the on-axis RMS values, the yellow background represents a T-IOL decentration in the Y-axis direction and the grey background a decentration in the X-axis direction.

Figure 6 shows the astigmatism values for the T-IOLs with CYL +1.50, +4.50 and +7.50 D for rotation in both directions (positive and negative). Although defocus and coma were also analyzed, they are not shown due to their minimal or zero variation with rotation. The variation of astigmatism is shown to be linear with rotation and symmetrical, irrespective of whether the rotation is applied in the negative or positive direction. As an example, for the atoric Lens B design with CYL +1.50 D, the astigmatism with a rotation of 15° is 0.156 µm, while for the CYL +7.50 D and the same rotation, the astigmatism obtained is 0.786 µm.

3.2. *Experimental analysis*

Figure 7 shows the MTF experimental data for the different T-IOLs manufactured with decentration, as measured on the PMTF optical bench using a spherical artificial cornea with +0.295 µm SA for a +6.00 mm entrance pupil diameter, following ISO specifications. Decentration was applied on the vertical and horizontal axes. Note that the MTF values in the horizontal (vertical) directions are not shown in Fig. 7 for vertical (horizontal) decenter directions, respectively, due to the fact that only one IOL meridian is being compensated by the rotationally symmetric artificial cornea during PMTF measurements, therefore their values are not useful for the study of image quality. As was predicted by numerical calculations (Fig. 1), the MTF degradation was found to

Biomedical Optics EXPRESS

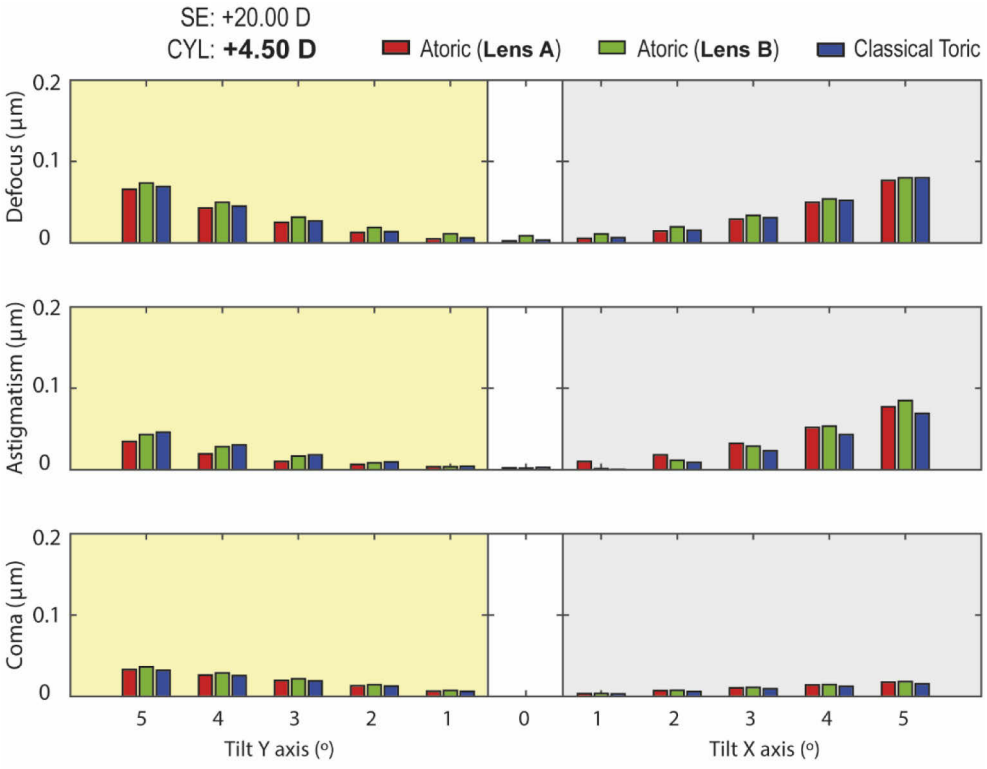

Fig. 5. Numerical results of the RMS defocus, astigmatism and coma for tilt for the different T-IOL designs with a +4.50 D cylinder, measured with a 3.00 mm diameter pupil. The white background represents the on-axis RMS values, the yellow background represents a T-IOL tilt in the Y-axis direction, and the grey background a tilt in the X-axis direction.

be dependent on the IOL design. For all the CYL powers analysed, atoric Lens A is the only one that obtains the highest MTF value for the centered position, with this value being higher than 0.43. For atoric Lens B and classical toric lenses, the MTF in the on-axis position is never higher than the limit established in ISO 11979-2 for any CYL power analysed. However, atoric Lens A is the most affected by decentration, with larger decentrations resulting in larger MTF decreases. In addition, the MTF is more affected by decentration at higher CYL values. Thus, for a CYL of +1.50 D, the MTF is already less than 0.43 for a 0.75 mm decentration when applied in both axes. For a CYL of +4.50 D, the MTF is less than 0.43 with a 0.50 mm decentration in the horizontal axis and 0.25 mm in the vertical one, and for a CYL of +7.50 D, the MTF is already lower with a decentration of 0.25 mm. The atoric Lenses B and the classical toric lenses barely suffer any alteration in their MTF upon decentration.

Figure 8 represents the TF-MTF for the toric lenses manufactured when placed in a nominal non-rotated position. The results for the different cylinders are shown in each row. For each cylinder, the axial scanning of the TF-MTF was changed to allow for analysis of the two foci with every T-IOL. The data shown in Fig. 8 were processed and compiled in Table 4 to facilitate analysis.

According to standard ISO 11979-2 [17], the acceptance criterion as regards the tolerance of the SE in a manufactured T-IOL of +20.00 D is ±0.4 D [17]. It can be seen from Table 4 that all T-IOLs manufactured meet this specification. The acceptance criteria for the CYL power with cylinders of +1.50, +4.50 and +7.50 D is ±0.3, ±0.4 and ±0.5 D respectively [17]. Once again,

Biomedical Optics EXPRESS

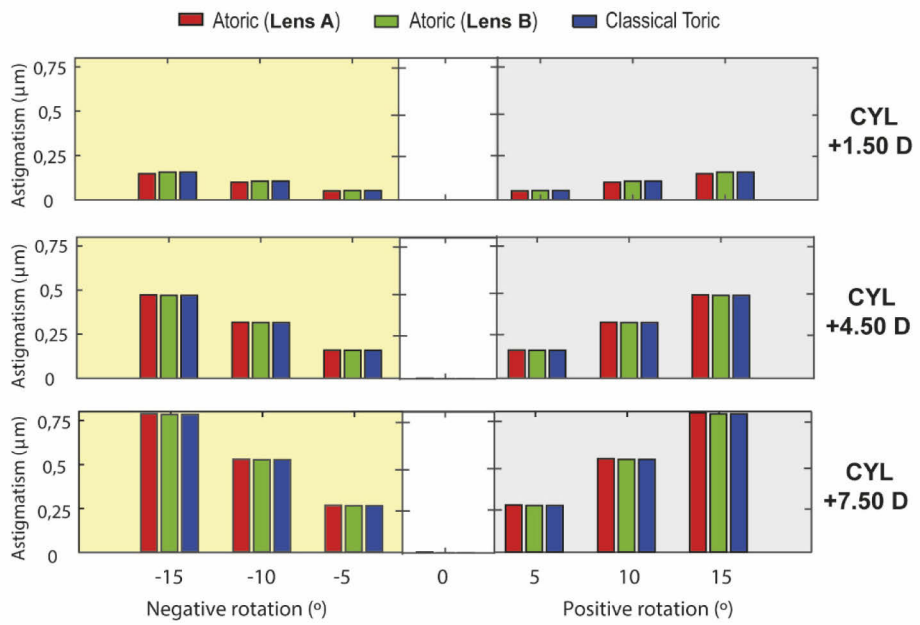

Fig. 6. Numerical results of the RMS astigmatism for the different T-IOL designs for each cylinder upon rotation, measured with a 3.00 mm diameter pupil. The white background represents the on-axis RMS values, the yellow background represents a T-IOL rotation in the negative direction, and the grey background a rotation in the positive direction.

Table 4. Experimental SE, CYL and MTF results for each T-IOL prototype manufactured, as measured using the PMTF optical bench. MTF is calculated for an object of 100 cycles/mm. Blue columns show the resulting SE and CYL for the lenses, as obtained from the individual power of each meridian for the maximum MTF. The MTF values highlighted in red do not meet the requirements of standard ISO 11979-2.

T-IOL (SE = +20.00 D)	Design	X focus		Y focus		SE (D)	CYL (D)
		Power (D)	MTF	Power (D)	MTF		
+1.50 D CYL	Atoric Lens A	19.11	0.55	20.35	0.54	19.73	1.24
	Atoric Lens B	18.97	0.43	20.64	0.40	19.81	1.67
	Classical Toric	19.20	0.41	20.54	0.44	19.87	1.34
+4.50 D CYL	Atoric Lens A	17.41	0.54	21.96	0.51	19.68	4.55
	Atoric Lens B	17.64	0.42	21.87	0.36	19.76	4.23
	Classical Toric	17.68	0.40	22.23	0.33	19.96	4.55
+7.50 D CYL	Atoric Lens A	16.19	0.46	23.66	0.52	19.93	7.47
	Atoric Lens B	16.10	0.37	23.77	0.42	19.94	7.67
	Classical Toric	16.34	0.35	23.34	0.35	19.84	7.00

Biomedical Optics EXPRESS

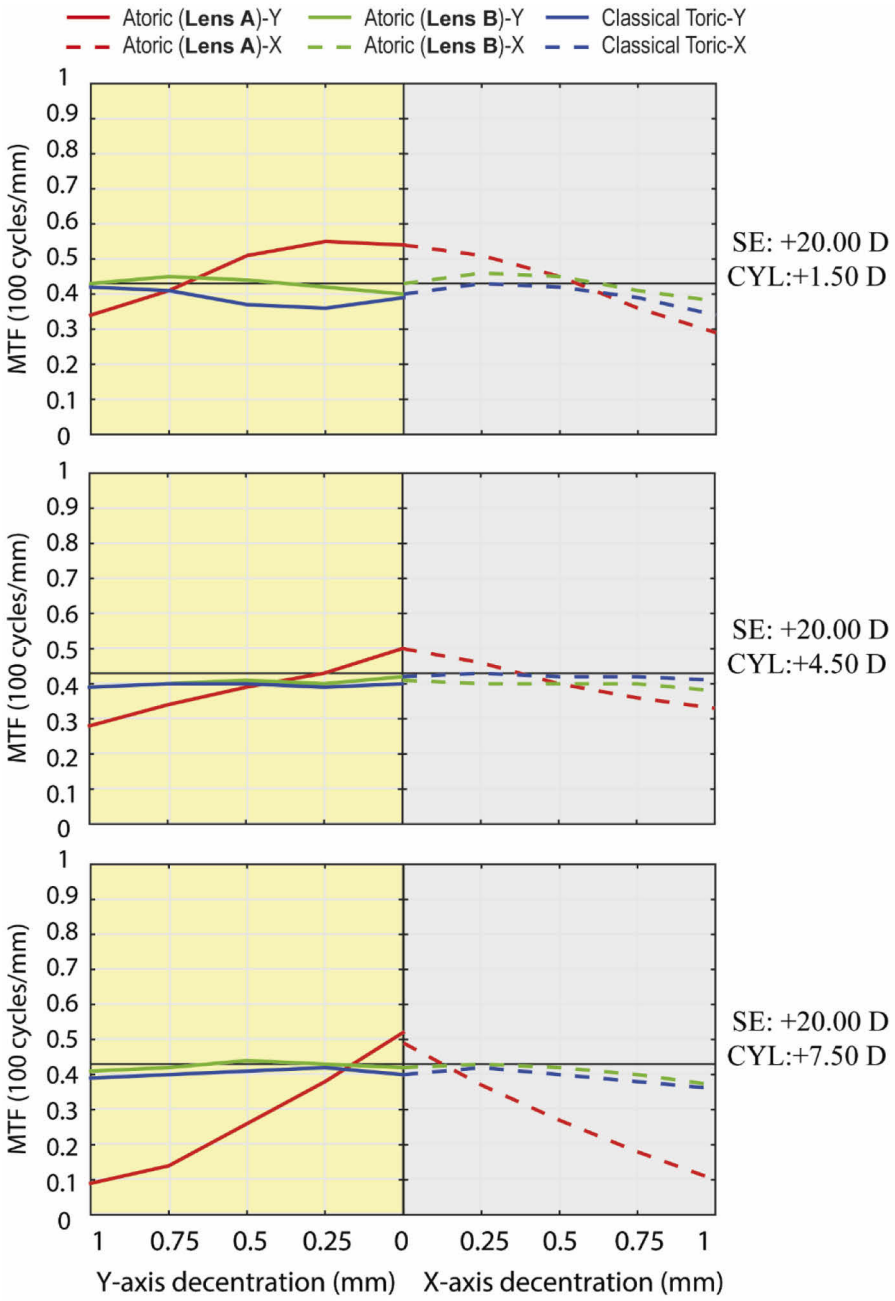

Fig. 7. Experimental MTF-Y (continuous line) and MTF-X (dashed line) values for the different T-IOL designs as a function of decentration, with a 3.00 mm pupil diameter and 100 cycles/mm for the different cylinder diopters. Testing was performed *in vitro* using the PMTF optical bench. Decentration was applied in the vertical direction (left side of the graph) and the horizontal direction (right side of the graph). The horizontal line represents an MTF value of 0.43, the tolerance limit established in ISO 11979-2 [17].

Biomedical Optics EXPRESS

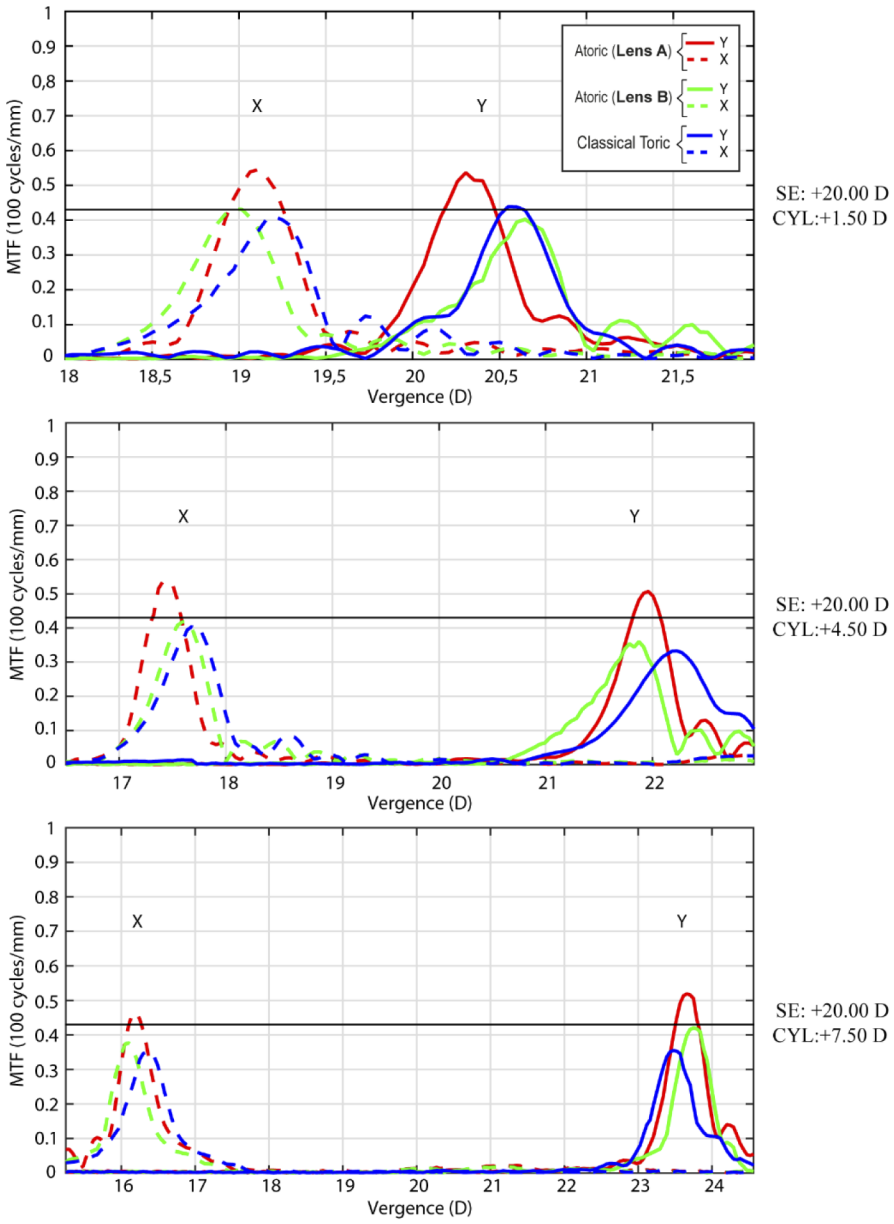

Fig. 8. Experimental TF-MTF (3.00 mm pupil diameter and 100 cycles/mm) for the different T-IOL designs manufactured in the on-axis position, as tested *in vitro* using the PMTF optical bench. TF-MTF-X (dashed lines) TF-MTF-Y (continuous lines). The results for different cylinder diopters are shown on each graph. For the T-IOLs with +1.50 D CYL, axial scanning was performed from 18.00 to 22.00 D. For the T-IOLs with +4.50 D CYL, axial scanning was performed from 16.50 to 23.00 D, and for the T-IOLs with +7.50 D CYL, axial scanning was performed from 15.25 to 24.50 D. The horizontal line represents an MTF value of 0.43, the tolerance limit established in ISO 11979-2 [17].

Biomedical Optics EXPRESS

all the T-IOLs manufactured meet these specifications. The atoric Lens A gave an MTF value higher than 0.43 for all cylinders manufactured, whereas the atoric Lens B and the classical toric lens gave MTF values lower than 0.43 for some or both meridians.

4. Discussion

To the best of our knowledge, this is the first study in which different aspheric designs of T-IOLs with different values of SA and with different amounts of astigmatism (low, moderate and high) have been designed and manufactured for a specific model cornea with astigmatism. The impact of rotation and tilt on the optical quality were evaluated theoretically by means of simulated ray tracing on an astigmatic eye model, while the effect of decentration was evaluated both theoretically and experimentally (using a PMTF optical bench).

As can be seen from the numerical simulations with the model eye, the optical quality (in terms of MTF-Y and MTF-X) is dependent on the degree of SA correction for the decentration (see Fig. 1). However, the effect of IOL tilt (see Fig. 2) is less dependent on the T-IOL design than the effect of IOL decentration, for the tilt and decentration values. The results of the present study show that the different designs have no impact on the optical quality when T-IOLs are rotated (see Fig. 3). These results agree with those shown in Table 3, where the sphero-cylindrical refraction error of the astigmatic cornea and T-IOL system with a 15° rotation of the T-IOL is shown.

In a perfectly centered and non-tilted position, the atoric Lens B (with an aberration-free design) and the classical toric IOL provide a worse MTF for the three cylinder values than the aspherical and negative SA lens (atoric Lens A). However, atoric Lens B and the classical toric lens maintained their optical quality over the entire decentration range analyzed. The trend indicated in these numerical results was also confirmed experimentally upon measurement using the PMTF system (see Fig. 7). These findings are in good agreement with the results reported in several previous experimental studies [25,26,27,28] in which rotationally symmetric monofocal IOLs with different dioptric powers and different degrees of SA were evaluated. In those studies, which were performed numerically, experimentally or as a combination of the two, different artificial corneas with different degrees of SA were used. Kim *et al.* [8] evaluated the effect of decentration (0.00 to 1.00 mm, in 0.1 mm steps) and rotation (0 to 16°, in 2° steps, and 20 to 32°, in 4° steps) of four commercial aspheric T-IOLs experimentally in terms of image quality. The artificial cornea had an SA of +0.189 μm for a 6.00 mm entrance pupil diameter. The SE of the lenses was +21.0 and +21.5 D, with CYL values of +2.00 and +2.25 D, respectively. These authors found that, for a decentration of 1.00 mm, the lenses with a CYL of +2.25 D and negative SA showed a decrease in optical quality, while the aberration-free lenses were almost decentration independent. Similarly, Pérez-Vives *et al.* [15] studied the optical quality of the same design of T-IOLs [Acrysof IQ Toric IOLs (SN6AT)] with different cylinder powers (+1.50, +2.25 and +3.30 D) experimentally upon decentration. These authors evaluated T-IOLs of different SE powers (+15.00, +20.00 and +23.50 D) using an NIMO instrument (Lambda-X, Belgium), which uses a customized wavefront to simulate the cornea during the measurements. The model SN6AT was a T-IOL with negative SA. The decentrations analyzed (0.3 and 0.6 mm) exhibited a substantial decrease in MTF for larger decentration.

As can be noted from Fig. 1, the numerically calculated behavior of MTF with decentration is the same irrespective of the astigmatism compensation degree. This result is not unexpected because MTF calculations were obtained from eye models with customized toric corneas to fully compensate the astigmatism of the IOL. Once the IOL's astigmatism is neutralized, it is straightforward to realize that differences in behavior due to decentration can only be due to differences in spherical aberration for each IOL design.

With regard to the experimental results, a study of the MTF values obtained using the PMTF bench (Fig. 7) showed that MTF decay with misalignment is slightly higher at higher IOL astigmatism. This becomes more evident for the T-IOL with CYL +7.50 D in comparison

Biomedical Optics EXPRESS

with those with CYL +1.50 and +4.50 D. The apparent contradiction between the numerical calculations (Fig. 1) and experimental measurements (Fig. 7) can be explained by the fact that these results were not obtained under the same conditions. Thus, in contrast to the full astigmatism compensation for the ray tracing calculation, the MTF values obtained in the PMTF were measured for a rotationally symmetrical cornea (as required by standard ISO 11979-2 [17]), therefore the IOL astigmatism was not fully compensated. As a different residual astigmatism is present during each measurement series, it is not unexpected to obtain different MTF values for IOLs with different astigmatism. This result should serve as a warning to take careful note of the experimental conditions before extrapolating conclusions applied to the real environment. Likewise, it also suggests the need to develop astigmatic model corneas to measure T-IOLs on optical benches. As mentioned above, the effect of IOL tilt was less dependent on the IOL design (see Fig. 2). Similar results were found in other studies with monofocal IOLs with different degrees of SA [25,26,27,28]. Thus, Felipe *et al.* [29] reported that the MTF decay due to aberrations was more sensitive to rotation than tilt. With a tilt >1°, the average modulation remains virtually unchanged. This result agrees with our findings. That study [29] was performed experimentally using a commercial T-IOL with an artificial cornea with no astigmatism, and the authors used crossed lines to measure MTF in both directions.

The rotation studied here causes an important deterioration in optical quality compared with decentration and tilt. As such, the effect of IOL rotation is less dependent on the IOL design. However, the degree of cylinder is crucial when the T-IOL is rotated because there is a strong positive correlation between the amount of degradation (in terms of MTF-Y and MTF-X) and the degree of cylinder power (see Fig. 3 and Table 3). A similar result was found by Ruiz-Alcocer *et al.* [31]. Our results show that the MTF decreases drastically with rotation, resulting in an MTF of less than 0.1 at a rotation of 5° in all T-IOL designs for the cylinders +4.50 and +7.50 D. Tognetto *et al.* [14] found that a rotation greater than 10° affected the image quality and a rotation of 45° caused a 100% loss of any toric correction. However, other studies [3,30] reported that the magnitude of total astigmatism after a 30.00° rotation in the T-IOL is equivalent to the pre-existing corneal astigmatism. Kim *et al.* [8] reported that only a conic toric IOL with an aberration-free design showed a superior MTF value compared with the other T-IOLs for a 15.00° rotation.

Our results show that the IOL decentration and tilt increase wavefront aberrations (see Figs. 4 and 5). In general, RMS defocus, astigmatism and coma increase with decentration depending on the degree of SA correction produced by the T-IOL. The relation between tilt and RMS defocus, astigmatism and coma are less dependent on the IOL design. Our results in this regard agree with those obtained by other authors [27,28,29].

Figure 8 shows the TF-MTF curves measured for all the T-IOLs manufactured in a centered and untilted position when an artificial cornea with +0.295 µm SA (for a 6.00 mm entrance pupil diameter) was used in the PMTF optical bench. With this scenario, Table 4 shows the atoric Lens A to be the only T-IOL design with MTF values higher than 0.43 for all cylinders, which is the acceptance criterion for the optical quality of manufactured lenses established in standard ISO 11979-2 [17]. Nevertheless, it is important to note that this experimental result does not imply that the atoric Lens A design was the only T-IOL manufactured according to the ISO criterion. Indeed, after the manufacturing process, it was checked experimentally that all T-IOL samples used in this work fulfilled the ISO tolerance criterion. According to ISO 11979-2 [17], these experimental optical quality checks were carried out with different artificial cornea models depending on the T-IOL design: a cornea with average positive SA was used to measure the TF-MTF curves for T-IOLs manufactured with atoric A-designs (SA negative), while a model cornea with zero SA was used to obtain the TF-MTF curves for T-IOLs manufactured with zero (B-design) or quasi-zero SA (classic toric) designs. In this situation, the atoric Lens B and the

Biomedical Optics EXPRESS

classic toric design have MTF values higher than 0.43. For the sake of brevity, these experimental PMTF measurements are not included in this text.

It can be seen from Fig. 1 that the behaviors of MTF upon decentration for the atoric IOL B and the classical toric IOL are very similar. This result is expected according to the third-order theory framework for pupil-decentered optical systems published by Wang *et al.* [32] taking into account the fact that these two IOL designs also have similar fourth-order aberration values (see Table 2).

In this work, an MTF of 100 cycles/mm has been used to determine the preclinical optical quality of different T-IOLs in the presence of decentration, tilt and rotation. The MTF is commonly used to compare different IOL designs under different conditions [33] and to evaluate the clinical outcomes [34]. However, some types of IOLs on the market offer poor MTF values for a particular spatial frequency in the optical bench but provide good visual acuity to patients (multifocal lenses, trifocal lenses and extended depth-of-focus lenses). For instance, Alarcon *et al.* [35] have proposed several pre-clinical metrics based on the evolution of MTF from 0 to 50 cycles/mm. In our study we used the MTF at a single spatial frequency as this is the acceptance criterion established in standard ISO 11979-2 [17]. It is possible that if we had used other metrics based on MTF integration in a range of spatial frequencies, our results would have been different due to the contribution of SA for such frequencies. However, no significantly different performances are expected for our classical toric or atorical tested IOL designs for the different misalignments.

5. Conclusions

In conclusion, using the range and T-IOL designs analysed, it has been shown that a lens with an aberration-free design (atoric Lens B) best maintains the optical quality upon decentration in both the numerical and experimental analyses (following the requirements specified in ISO 11979-2), whereas for tilt tolerance all T-IOL designs tested behave in a very similar manner. Moreover, the expected CYL power dependence of optical quality on rotation errors was also verified numerically in terms of MTF 100 cycles/mm, with this loss being more acute at higher CYL powers. As was also found in the tilt case, this behavior was design-independent.

The results obtained in this study may help surgeons to better understand T-IOL optical performance and to select the best IOL for a patient in order to improve surgical outcomes. The results suggest that if alignment cannot be guaranteed in cases with anatomic anomalies (e.g. zonular instability or weakness) or factors that can cause IOL misalignment (e.g. a large capsulorhexis, incongruence between bag diameter and overall IOL diameter, asymmetric capsule coverage), aberration-free T-IOLs (atoric Lens B) may be the best option for a specific patient in order to provide acceptable imaging even with some decentration and tilt. In T-IOLs with negative spherical aberration, the IOL decentration increased coma aberrations, which may negatively influence visual performance.

Furthermore, the comparison of PMTF normative experimental measurements and numerically simulated real conditions with misalignments also allowed us to conclude that, specifically for toric IOLs, normative optical quality measurements for T-IOLs do not always lead to the same exact conclusions as the simulated real environment. This was the case, for example, for the independence of MTF quality impairment with misalignment as a function of the CYL power, which was observed from numerical calculations, in comparison with the MTF measurements obtained with a PMTF for real T-IOLs. We consider that the cause of these differences, and their possible practical consequences, deserves further study in the future.

With regard to the limitations of this work, it is noted that the optical quality was studied with monochromatic light under fovea-centered conditions (under both numerical and experimental conditions), therefore our results do not include the effect of longitudinal or transversal chromatic aberration [36,37] or geometrical aberration effects due to kappa angle [38,39,40], respectively.

Biomedical Optics EXPRESS

However, due to the fact that the main nature of chromatic aberration in a singlet refractive element lens comes from the material composition, a significantly different image trend performance between the toric or atorical IOL designs tested herein is not expected. Likewise, the astigmatic and aspherical surface was on the anterior surface of the IOLs and the aspherical lenses were designed with a pure biconical surface. Further studies may involve other aspherical designs [41,42], with an anterior and posterior aspheric surface and with the cylinder distributed on both.

Funding. Ministerio de Ciencia, Innovación y Universidades (Grant DPI2017-84047-R, Grant PID2020-114311RA-I00); Gobierno de Aragón (Grant E44-20R, Grant T24-20R); Ministerio de Economía y Competitividad (Grant DI-16-08888).

Acknowledgements. The authors acknowledge AJL Ophthalmic S.A. (Spain) for manufacturing the proof-of-concept T-IOLs used in this study.

Disclosures. The authors declare no conflicts of interest.

Data Availability. Data underlying the results presented in this paper are not publicly available at this time but may be obtained from the authors upon request.

References

1. S. Poler, "Intraocular lens with astigmatism correction," U.S. patent, 4,277,852A (21 January 1981).
2. L. Kessel, J. Andresen, B. Tendal, D. Erngaard, P. Flesner, and J. Hjortdal, "Toric Intraocular lenses in the correction of astigmatism during cataract surgery: a systematic review and meta-analysis," Ophthalmology (Philadelphia) **123**(2), 275–286 (2016).
3. K. Shimizu, A. Misawa, and Y. Suzuki, "Toric intraocular lenses: correcting astigmatism while controlling axis shift," J. Cataract Refractive Surg. **20**(5), 523–526 (1994).
4. D.M. Lieberman, "Method of offsetting postoperative astigmatism with an intraocular lens," U.S. patent, 4,512,039A (24 May 1985).
5. P.J. Nielsen, "Prospective evaluation of surgically induced astigmatism and astigmatic keratotomy effects of various self-sealing small incisions," J. Cataract Refractive Surg. **21**(1), 43–48 (1995).
6. H.B. Grabow, "Early results with foldable toric IOL implantation," Eur. J. Implant. Refract. Surg. **6**, 177–178 (1994).
7. M. Chehade and M.J. Elder, "Intraocular lens materials and styles: A review," Aust. N.Z.J. Ophthalmol. **25**(3), 255–263 (1997).
8. M.J. Kim, Y.S. Yoo, C.K. Joo, and G. Yoon, "Evaluation of optical performance of 4 aspheric toric intraocular lenses using an optical bench system: Influence of pupil size, decentration, and rotation," J. Cataract Refractive Surg. **41**(10), 2274–2282 (2015).
9. X. Zhu, J. Meng, W. He, X. Rong, and Y. Lu, "Comparison of the rotational stability between plate-haptic toric and C-loop haptic toric intraocular lenses in myopic eyes," J. Cataract Refractive Surg. **46**(10), 1353–1359 (2020).
10. J. Mendicute, C. Irigoyen, J. Aramberri, A. Ondarra, and R. Montés-Micó, "Foldable toric intraocular lens for astigmatism correction in cataract patients," J. Cataract Refractive Surg. **34**(4), 601–607 (2008).
11. F. Ucar and M. Ozcimen, "Can toric IOL rotation be minimized? Toric IOL-capsular tension ring suturing technique and its clinical outcomes," Semin. Ophthalmol. **14**(3), 378–382 (2021).
12. N. Garzón, F. Poyales, B. Ortíz de Zárate, J.L. Ruiz-García, and J.A. Quiroga, "Evaluation of rotation and visual outcomes after implantation of monofocal and multifocal toric intraocular lenses," J. Refract. Surg. **31**(2), 90–97 (2015).
13. K. Miháltz, M. Lasta, M. Burgmüller, P.V. Vécsei-Marlovits, and B. Weingessel, "Comparison of two toric IOLs with different haptic design: optical quality after 1 year," J. Ophthalmol. **2018**, 1–7 (2018).
14. D. Tognetto, A.A. Perrotta, F. Bauci, S. Rinaldi, M. Antonuccio, F.A. Pellegrino, G. Fenu, G. Stamatelatos, and N. Alpins, "Quality of images with toric intraocular lenses," J. Cataract Refractive Surg. **44**(3), 376–381 (2018).
15. C. Pérez-Vives, T. Ferrer-Blasco, D. Madrid-Costa, S. García-Lázaro, and R. Montés-Micó, "Optical quality of aspheric toric intraocular lenses at different degrees of decentering," Graefes Arch. Clin. Exp. Ophthalmol. **252**(6), 969–975 (2014).
16. B. Zhang, J.X. Ma, D.Y. Liu, Y.H. Du, C.R. Guo, and Y.X. Cui, "Optical performance of toric intraocular lenses in the presence of decentration," Int. J. Ophthalmol. **8**(4), 730–735 (2015).
17. "Ophthalmic implants – intraocular lenses. Part 2: optical properties and test methods," ISO 11979-2:2014.
18. D.A. Atchison, "Optical models for human myopic eyes," Vision Res. **46**(14), 2236–2250 (2006).
19. P.A. Piers, S. Norrby, and M. Ulrich, "Eye models for the prediction of a contrast vision in patients with new intraocular lens designs," Opt. Lett. **29**(7), 733–735 (2004).
20. J.T. Holladay, P.A. Piers, G. Koranyi, M. van der Mooren, and S. Norrby, "A new intraocular lens design to reduce spherical aberration of pseudophakic eyes," J. Ref. Surg. **18**(6), 683–691 (2002).
21. D. Meister, "Principles of atoric lens design," Lens Talk. **27**(3), 1–4 (1998).
22. American National Standard ANSI Z80.28-2017: Ophthalmics – Methods of reporting optical aberrations of eyes (2017).

Biomedical Optics EXPRESS

23. A. Guirao and D.R. Williams, "A method to predict refractive errors from wave aberration data," Optom. Vis. Sci. **80**(1), 36–42 (2003).
24. D.R. Iskander, B.A. Davis, M.J. Collins, and R. Franklin, "Objective refraction from monochromatic wavefront aberrations via Zernike power polynomials," Oph Phys Optics **27**(3), 245–255 (2007).
25. J. Pérez-Gracia, A. Varea, J. Ares, J.A. Vallés, and L. Remón, "Evaluation of the optical performance for aspheric intraocular lenses in relation with tilt and decenter errors," PLoS One **15**(5), e0232546 (2020).
26. T. Eppig, K. Scholz, A. Löffler, A. Messner, and A. Langenbucher, "Effect of misalignment and tilt on the image quality of aspheric intraocular lens designs in a model eye," J. Cataract Refractive Surg. **35**(6), 1091–1100 (2009).
27. P. Pérez-Merino and S. Marcos, "Effect of intraocular lens misalignment on image quality tested in a custom model eye," J. Cataract Refractive Surg. **44**(7), 889–896 (2018).
28. T. Lawu, K. Mukai, H. Matsushima, and T. Senoo, "Effects of misalignment and tilt on the optical performance of 6 aspheric intraocular lens designs in a model eye," J. Cataract Refractive Surg. **45**(5), 662–668 (2019).
29. A. Felipe, J.M. Artigas, A. Díez-Ajenjo, C. García-Domene, and C. Peris, "Modulation transfer function of a toric intraocular lens: evaluation of the changes produced by rotation and tilt," J. Refract. Surg. **28**(5), 335 (2012).
30. J.T. Holladay and D.D. Koch, "Residual astigmatism with toric intraocular lens misalignment," J. Cataract Refractive Surg. **46**(8), 1208–1209 (2020).
31. J. Ruiz-Alcocer, A. Lorente-Velázquez, P. de Gracia, and D. Madrid-Costa, "Optical tolerance to rotation of trifocal toric IOLs as a function of the cylinder power," Eur. J. Ophthalmol. **31**(3), 1007–1013 (2021).
32. J. Wang, B. Guo, Q. Sun, and Z. Lu, "Third-order aberration fields of pupil decentered optical systems," Opt. Express **20**(11), 11652 (2012).
33. F. Vega, F. Alba-Bueno, M. S. Millán, C. Varón, M. A. Gil, and J. A. Buil, "Halo and through-focus performance of four diffractive multifocal intraocular lenses," Invest. Ophthalmol. Vis. Sci. **56**(6), 3967–3975 (2015).
34. X. Cheng, A. Bradley, and L.N. Thibos, "Predicting subjective judgment of best focus with objective image quality metrics," J. Vis. **4**(4), 310–321 (2004).
35. A. Alarcon, C. Canovas, R. Rosen, H. Weeber, L. Tsai, K. Hileman, and P. Piers, "Preclinical metrics to predict through-focus visual acuity for pseudophakic patients," Biomed. Opt. Express **7**(5), 1877–1888 (2016).
36. L.N. Thibos, A. Bradley, D.L. Still, X. Zhang, and P.A. Howart, "Theory and measurement of ocular chromatic aberration," Vision Res. **30**(1), 33–49 (1990).
37. S. Marcos, S.A. Burns, E. Moreno-Barriuso, and R. Navarro, "A new approach to the study of ocular chromatic aberrations," Vision Res. **39**(26), 4309–4323 (1999).
38. Y. Le Grand and S. G. El Hage, *Physiological Optics, Springer Series in Optical Sciences* (Springer, 1980).
39. J. Tabernero, P. Piers, and P. Artal, "Intraocular lens to correct corneal coma," Opt. Lett. **32**(4), 406–408 (2007).
40. S. Marcos, P. Rosales, L. Llorente, S. Barbero, and I. Jiménez-Alfaro, "Balance of corneal horizontal coma by internal optics in eyes with intraocular artificial lenses: evidence of a passive mechanism," Vision Res. **48**(1), 70–79 (2008).
41. G.W. Forbes, "Shape specification for axially symmetric optical surfaces," Opt. Express **15**(8), 5218–5226 (2007).
42. B. Chassagne and L. Canioni, "Analytical solution of a personalized intraocular lens design for the correction of spherical aberration and coma of a pseudophakic eye," Biomed. Opt. Express **11**(2), 850–866 (2020).